# Effect of particle size oscillations on drift and diffusion along a periodically corrugated channel

Yu. A. Makhnovskii*

*Topchiev Institute of Petrochemical Synthesis, Russian Academy of Sciences, Leninsky Prospect 29, Moscow 119991, Russia*

(Received 29 October 2018; revised manuscript received 25 January 2019; published 5 March 2019)

We study diffusive transport of a particle in a channel with periodically varying cross-section, occurring when the size of the particle periodically switches between two values. In such a situation, the entropy potential, which accounts for the area accessible for diffusion particle, varies both spatially (along the channel axis) and temporally. This underlies the complex interplay between different timescales of the system and leads to novel dynamic regimes. The most notable observations are: emergence of directed motion (in case of asymmetric channel) and resonant diffusion, both controlled by the switching frequency. Resonantlike behaviors of the drift velocity and the effective diffusion coefficient are shown and discussed. Based on heuristic arguments, an approximate analytical treatment of the transport process is proposed. As a comparison with the results obtained from Brownian dynamics simulations indicates, this approach provides a satisfactory way to handle the problem analytically.

DOI: 10.1103/PhysRevE.99.032102

## I. INTRODUCTION

Diffusive transport in corrugated channels is ubiquitous in nature and technology. Among obvious examples are such diverse phenomena as solute transport in porous solids and various complex media [1], transportation of ions through channels in membranes [2], sorting particles by size [3], controlled drug delivery [4], translocation of polynucleotides in living tissues [5], and entropic rectification [6,7], just to mention a few of them. Research into various aspects of the subject has thrived over the past decades, motivated to a large extent by several applications in molecular biology and nanoscale engineering. Numerous theoretical predictions surveyed in exhaustive review articles [5,8–10] are supported by experimental evidence [11–13].

A sequence of cross-sectional irregularities such as channel expansions and constrictions may dramatically affect both equilibrium and kinetic properties of the particle transport. Although the channel geometry and transported species vary from system to system, the basic physics involved is universal. It stems from a variation of the space accessible to particles along the propagation direction. The inhomogeneity in the confining space suggests use of a position-dependent entropy potential in reduced dimensions [14,15], so the transport in corrugated channels evolves through entropy barriers and entropy wells. Most of the studies invariably assumes an overdamped particle dynamics. For specific situations, the impact of inertia on biased diffusion regulated by entropic barriers can become, however, of salient importance [16].

Entropic effects lead to novel dynamical regimes which have a global occurrence in soft matter and biological systems. The best-studied example is forced and force-free entropic transport in quasi-one-dimensional (1D) structures, which exhibits striking, sometimes counterintuitive, features in certain geometry designs [9,17–20]. Another point of current research is focused on the question of how hydrodynamics affects diffusion through entropic barriers [12,21]. An asymmetric channel corrugation offers a means to rectify fluctuations brought about by a source of unbalance [6,7,11,21–29]. Both rocking [11,22,23] and flashing [24–27] scenarios have been proposed to rectify the particle motion in the main transport direction via the entropy potential. The phenomenon of entropic rectification has attracted enormous interest because it not only provides a direct way to produce a controlled directed motion at submicron scale [8], but also can be useful for modeling the delivery of molecular products to their correct location within a cell [4,5], as well as for developing efficient methods of nanoparticle separation [3,21]. Entropic rectification of active particles may be used to sort the particles according to their self-propelled speeds [28]. Cooperative ratcheting via both a potential-energy and an entropy potential can significantly enhance the system response and, moreover, yield directed motion in situations where neither energetic nor entropic mechanisms operate on their own [29]. A non-trivial involvement of the size of a diffusing particle into dynamics of geometry influenced transport has been revealed [30–32].

The present paper addresses the question of how a time variation of the particle size affects its transport in a channel of varying cross-section. It should be remarked that a reversible, relatively large change in the size of nano-objects (macromolecules and molecular aggregates) triggered by an external stimulus (electric field, light, temperature, or PH) is well established and has various manifestations [33]. An excellent example is furnished by nanoparticles wholly composed of photochromic groups, the diameter of which decreases to almost one-half and recovers through the UV-induced cross-linking and cleavage of the cinnamate groups in the polymer backbone [34]. Another example is photo-responsive microgel particles, the reversible changes of which can be achieved by alternative UV–Vis light irradiations [35]. As a third example, it might be mentioned photo-driven

*yuam@ips.ac.ru

 

pulsating vesicles from self-assembled lipidlike azopolymers [36]. Thus, systems, where geometrically restricted particle diffusion is coupled with a time variation of the particle size, can potentially be realized experimentally.

To achieve the goal in question, we consider a particle diffusing in a 2D periodic channel. The particle size periodically switches between two values, in response to an external stimulus. This implies that the particle is subject to an oscillating entropy potential and, via the Stokes-Einstein relation, its diffusion coefficient oscillates in time. The interplay of the different timescales in the particle dynamics (such as the period of the size oscillation, the characteristic time of the system response, and the diffusion time) causes nontrivial transport behavior. This study exhibits the two main features of particle transport in a channel induced by its size oscillation: emergence of directed motion (in case of asymmetric channel) without any macroscopic force or gradient and resonant diffusion, both controlled by the switching frequency.

Directed transport of Brownian particles due to a time variation, deterministic or stochastic, of an asymmetric periodic potential (flashing ratchet mechanism [37]) is by now a well-established phenomenon observed in various nonlinear systems [5,6,8,24–27]. So the rectification scenario observed here is a specific realization of the flashing ratchet mechanism. The idea that particle size oscillations and asymmetry of environment conspire to produce directed motion has been recently proposed and discussed for periodic [26] and stochastic [27] variations of the particle size. The current study extends our previous work [26] to include the influence of the particle size oscillation on its diffusion behavior. Note that diffusion in a periodic potential is a fundamental problem of long-standing and continuous interest. At equilibrium, the free diffusion is hindered by energy or entropy barriers [38]. Out of equilibrium, diffusion may exhibit counterintuitive behavior: When a periodic potential is perturbed by a static bias force [39], the diffusion rate shows a giant enhancement (over the rate of free diffusion) [9,40], or even diverge [6,19]; time-dependent driving leads to the resonant diffusion acceleration, as predicted theoretically [41] and observed experimentally [42]. This work provides an example of resonant diffusion induced by space- and time-varying geometry.

The organization of the paper is as follows: In Sec. II, we introduce the model and the basic quantities of interest, namely, the drift velocity and the effective diffusion coefficient, as well as outline our approach to modeling the particle transport. Section III reports and discusses our main findings: the results obtained from extensive Brownian dynamics simulations for the quantities of interest (Secs. III A and III B), the approximate analytical treatment of the problem based on a few heuristic arguments capturing the basic physics of the model (Sec. III C), and a comparison between the analytical predictions and the numerical results (Sec. III D). Finally, the major contributions of the present work are summarized in Sec. IV.

## II. THE MODEL

Consider a spherical particle diffusing in a 2D fluid-filled $L$-periodic channel, schematically shown in Fig. 1. The channel with bottleneck width $2a$ is symmetric about the $x$ axis. The upper and low confining zigzag walls, $y_u$ and $y_l$, are described by the periodic piecewise-linear function

$$y_u(x) = -y_l(x) = a + \begin{cases} k_1\bar{x}, & \bar{x} < C \\ k_2(L-\bar{x}), & \bar{x} \geqslant C \end{cases}, \quad (1)$$

where $k_1$ and $k_2$ are the slopes of the walls, $C = k_2L/(k_1+k_2)$ refers to the maximum channel width position, and $\bar{x}$ is defined via the module function $\bar{x} = x \mod L$. The left-right asymmetry of the model is brought about by the difference between $k_1$ and $k_2$.

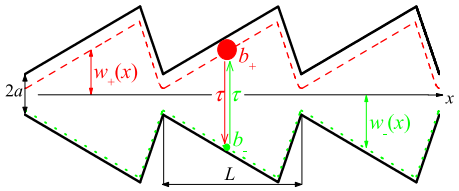


FIG. 1. Schematic illustration of a 2D $L$-periodic channel, with bottleneck width $2a$. The channel walls confining the motion of a spherical Brownian particle are determined by Eq. (1). The particle radius alternates between two values, $b_+$ and $b_-$, every time interval $\tau$. The dashed and dotted lines indicate the limiting positions of the particle center within the channel in the $+$ and $-$ states, respectively. The half-width of the effective region accessible for diffusion, $w_\pm(x)$, is defined by Eq. (3).

The suspended particle possesses two states, $+$ and $-$, which differ by the particle radius, $b_+ < a$ and $b_- < a$ (for definiteness, let $b_+ > b_-$). When driven by an external periodic signal (with period $2\tau$), the states alternate every half period $\tau$. According to the Stokes-Einstein relation, the particle's diffusion coefficient also alternates between two values, $D_+$ and $D_- = (b_+/b_-)D_+$, and hence it is time periodic,

$$D(t) = \{(D_+ + D_-) + (D_+ - D_-)\,\mathrm{sgn}\,[\sin(\pi t/\tau]\}/2, \quad (2)$$

where $\mathrm{sgn}(t)$ denotes the sign function. We neglect rare spontaneous (thermal) interstate transitions, occurring without any external stimulus, which satisfy detailed balance and hence, by itself, cannot produce directed motion. Besides, the model leaves out additional complexities such as interactions among particles, particle wall interactions (apart from hard core repulsion), and back-reaction of the medium to the particle size changes (which implies not too large amplitude of the oscillation) to exhibit the effects under study in a most clear manner.

The region available for diffusion of a finite-size particle is smaller than the total area of the channel. An effective boundary restricting the particle motion is distant from the channel wall by the radius $b_+$ or $b_-$. The local half-width of the structures reduced in a such way reads

$$w_\pm(x) = a + \begin{cases} -\sqrt{b_\pm^2 - \bar{x}^2}, & 0 \leqslant \bar{x} < \varepsilon_\pm \\ k_1\bar{x} - b_\pm\sqrt{1+k_1^2}, & \varepsilon_\pm \leqslant \bar{x} < c_\pm \\ k_2(L-\bar{x}) - b_\pm\sqrt{1+k_2^2}, & c_\pm \leqslant \bar{x} < L - \delta_\pm \\ -\sqrt{b_\pm^2 - (L-\bar{x})^2}, & L - \delta_\pm \leqslant \bar{x} < L \end{cases}, \quad (3)$$

where $\varepsilon_\pm = (k_1/\sqrt{1+k_1^2})b_\pm$, $\delta_\pm = (k_2/\sqrt{1+k_2^2})b_\pm$, and $c_\pm = C + b_\pm(\sqrt{1+k_1^2} - \sqrt{1+k_2^2})/(k_1+k_2)$ refers to the maximum width position of the region accessible for the center of the particle of radius $b_\pm$. It is convenient to recast the original formulation of the model [a particle of periodically varying radius moving in a channel defined by Eq. (1)] into an equivalent one of a pointlike particle moving in a channel of periodically varying shape defined by Eq. (3). It might seem that in such formulation the model proposed here closely resembles those developed to analyze entropic effects in diffusive transport introduced by time-changing boundaries of a channel [24,25]. However, a wave of contraction and expansion moving on the fluid-filled channel wall gives rise to peristaltic pumping [43] which influence on the particle transport seems to dominate that of entropic effects. Additionally, here the particle's diffusion coefficient also oscillates in time, in contrast to Refs. [24,25].

The overdamped dynamics of the pointlike Brownian particle is governed by the equation

$$\frac{d\vec{r}}{dt} = \sqrt{2D(t)}\ \vec{\xi}\,(t), \tag{4}$$

supplemented by the condition of vanishing outflow at the walls of the effective channel, the half-width of which alternates between $w_+(x)$ and $w_-(x)$. Here $\vec{r}$ is the particle's position in the 2D channel, $D(t)$ is the time periodic function defined in Eq. (2), and $\vec{\xi}\,(t)$ denotes a 2D Gaussian white noise, with zero mean and correlation $\langle \xi_i(t)\xi_j(s)\rangle = \delta_{ij}\delta(t-s)$ for $i, j = x, y$. The focus is on the steady state reached at long times, when the particle's displacement, $\Delta x(t|\tau) = x(t|\tau) - x(0)$, significantly exceeds the channel period $L$ and the number of transitions between states is large enough. In this regime the particle's transport along the channel is conveniently characterized by the drift velocity $v(\tau)$ and the effective diffusion coefficient $\mathcal{D}(\tau)$, defined via the first two moments of $\Delta x(t|\tau)$:

$$v(\tau) = \lim_{t\to\infty} \frac{\langle \Delta x(t|\tau)\rangle}{t}, \tag{5}$$

$$\mathcal{D}(\tau) = \lim_{t\to\infty} \frac{\langle [\Delta x(t|\tau)]^2\rangle - \langle \Delta x(t|\tau)\rangle^2}{2t}. \tag{6}$$

The most common way to describing diffusive transport in a periodic channel of varying cross-section consists in reducing the dimensionality of the system, keeping only the main transport direction along the channel axis. With this approximation, the irregularity of the channel boundary $w_\sigma(x)$, $\sigma = +, -$ is accounted for by means of a periodic entropy potential $U_\sigma(x)$ and a properly chosen periodic $x$-dependent diffusion coefficient $D_\sigma(x)$. The effective half-width $w_\pm(x)$ can be interpreted as a Boltzmann weight of an entropy potential $U_\pm(x)$ felt by a walking particle due to collisions with the channel walls:

$$w_\pm(x) = a e^{-\beta U_\pm(x)}, \tag{7}$$

where $\beta = (k_B T)^{-1}$, $k_B$ is the Boltzmann constant, and $T$ is the temperature. The resulting kinetic equation for the effective 1D probability distribution, known as the Fick-Jacobs (FJ) equation [14,15,17], is the Smoluchowski equation, in which the potential of energetic origin is replaced by the entropy potential and the diffusion coefficient is position-dependent. One of the well-known results obtained from the Smoluchowski equation is the exact formula for the effective diffusion coefficient of a Brownian particle in a stationary periodic potential [38]. Analogously, it follows from the FJ equation that the effective diffusion coefficient of a point Brownian particle in a channel of the position-dependent width $2w_\pm(x)$ can be written as

$$\begin{aligned}\mathcal{D}_{\mathrm{FJ},\pm} &= \left[\int_0^L e^{-\beta U_\pm(x)}\,dx/L \int_0^L e^{\beta U_\pm(x)}/D_\pm(x)\,dx/L\right]^{-1} \\ &= \left\{\int_0^L w_\pm(x)\,dx/L \int_0^L 1/[w_\pm(x)D_\pm(x)]\,dx/L\right\}^{-1}.\end{aligned} \tag{8}$$

The second of Eq. (8) follows from the first in view of Eq. (7). The position-dependent diffusion coefficient $D(x)$ is introduced as a standard way to improve the accuracy of the FJ approximation. The problem of the correct $x$ dependence of $D(x)$ is still matter of debate (see, for example, [44]). Here we use a well tested expression suggested by Reguera and Rubí [15]:

$$D_\pm(x) = D_\pm\{1 + [dw_\pm(x)/dx]^2\}^{-1/3}. \tag{9}$$

The FJ approach, in general, and Eq. (8), in particular, provides a quite good approximation under the condition of fast equilibration in the transversal directions. This approximation is, however, invalid in systems with sharp geometries [18,19] or in the presence of external drive [6], where transverse relaxation can hardly be instantaneous. Moreover, in these cases the FJ approach does not guarantee even qualitative description of boundary effects in the diffusive transport. Thus, the model considered here can be formulated in terms of energetic flashing ratchet model (and hence admits an analytical treatment) only in some limiting cases (see below). Because of this, we choose Brownian dynamics simulations as the main research tool.

In this way, particle trajectories were generated by numerical integration of the dimensionless [45] stochastic equation of motion, equivalent to Eq. (4), using the forward Euler algorithm. The efficiency and quality of random number generator are critical in simulations. In this work, we used the ziggurat method [46], which is a reliable and fast method to produce random numbers with a very high period. The reflecting boundary condition at the wall of the effective channel was accomplished by mirroring back a trajectory inside the channel once it moves out of this region. The simulations were run at $a/L = 0.3$, $b_+/L = 0.25$, three values of $b_+/b_-$ (8.33, 4.0, 1.67), and switching time varying over several order of magnitude. The particle's motion was investigated both in the symmetric, $k_1 = k_2 = 0.504$, and asymmetric, $k_1 = 0.3$ and $k_2 = 1$, channels. The $k$ values were chosen in such a way that the calculated [analytically from Eq. (8) and numerically from simulations] effective diffusion coefficients of a point Brownian particle are the same in the symmetric and asymmetric channels. The drift velocity and the effective diffusion coefficient were calculated as the average over $10^5$ trajectories, following their definitions given in Eqs. (5) and (6), respectively. To get stable and accurate results, the time step

was taken to be $1.25\times10^{-7}$, which is much smaller than all other characteristic times in the problem. The number of steps varied from $1.2\times10^{8}$ (at $\tau \leqslant 0.05$) to $6\times10^{8}$ (at $\tau > 0.05$), so that the dimensionless observation time changed from 15 to 75 and each trajectory involved from hundreds to millions interstate transition events.

Along with numerical modeling, we present approximate analytical expressions for the drift velocity and effective diffusion coefficient. Their derivation is based on intuitive appealing arguments capturing the essential physics of the model. The analytical description not only clarifies the physical origin of the results obtained from the simulations but also yields reasonable quantitative predictions for the quantities of interest.

## III. RESULTS AND DISCUSSION

### A. Directed motion in an asymmetric channel

One of the main conclusions to emerge from the simulations is that variations of the particle size may produce directed motion, provided the shape of the channel is asymmetric. The greater the amplitude of the oscillation, $A = b_+ - b_-$, the stronger the effect. Just as in the case of 1D potential energy ratchets [37], the drift is directed toward the steeper slope, leading to a positive bias in the channel shown in Fig. 1, where $k_2 > k_1$. Note that a rocking driving pushes a Brownian motor (both energetic [37] and entropic [22,23]) in the opposite direction. The simulation data confirm the obvious fact that the drift is stronger for larger asymmetry and vanishes in the symmetric channel.

The important characteristic of any ratchet device is its response to a change in a frequency of an input signal. This is why the emphasis is made on the dependence of the drift velocity on the switching time, which serves as a control parameter. The results obtained from the simulations illustrate the dependence $v(\tau)$ in Fig. 2 for different values of $b_+/b_-$ ($b_+/L = 0.25$ is fixed). One can see that the drift velocity exhibits a resonancelike behavior versus the switching time. Such a behavior of $v(\tau)$ is inherent in Brownian motors driven by variations of the potential [37], and is qualitatively different from that observed for motors driven by variations of a force, where the velocity increases monotonically with $\tau$ [22,23,37].

The drift vanishes in the limiting regimes $\tau \to \infty$ and $\tau \to 0$. Its velocity exhibits a resonance regime close to its maximum at the intermediate values of the switching time. In the low-frequency regime the particle has enough time to equilibrate in each state, whereas in the opposite limit equilibrium is achieved in the averaged entropy potential, which rules out directed motion in both cases. As Fig. 2 indicates, the height and position of $v(\tau)$ depend on the oscillation amplitude $A = b_+ - b_-$. The stronger $A$, the greater the magnitude of the maximum. The position of the peak shifts to longer switching times as the amplitude decreases.

The particle size oscillation implies a time variation of the entropy potential. This underlies the motion inducing mechanism of purely entropic nature, by which the model operates as a Brownian motor [24,25]. The size oscillation is also accompanied by the variation of the particle diffusion coefficient, which by itself does not cause directed motion.

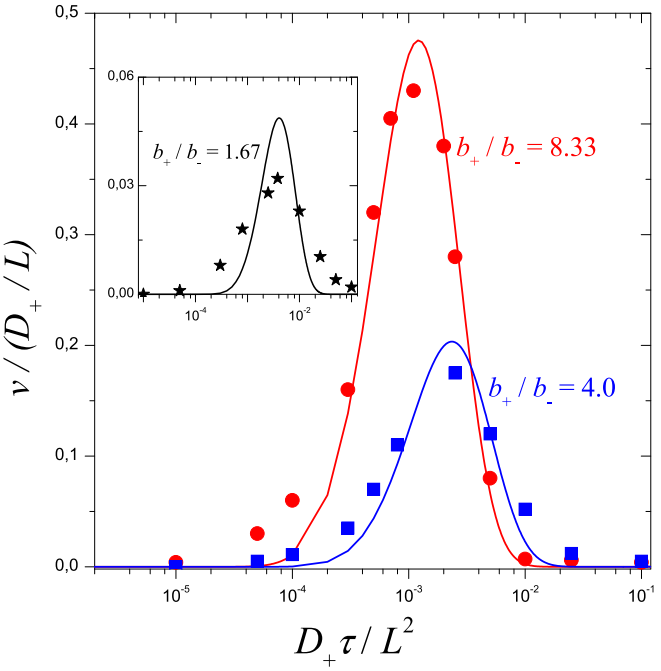


FIG. 2. Drift velocity in units $D_+/L$ vs. scaled switching time for different values of $b_+/b_-$ indicated by figures. Points, marked by symbols, are obtained from 2D Brownian dynamics simulations (the error of the data near the maximums is smaller than the size of the symbols used). The lines are calculated from Eq. (19). The inset compares numerical and analytical results for $b_+/b_- = 1.67$. The value of $b_+/L = 0.25$ is fixed; the dimensionless diffusion coefficients are $D_+ = 1$ and $D_- = b_+/b_-$.

However, as demonstrated in our earlier work [26], the variation of the diffusion coefficient, combined with the variation of the asymmetric entropy potential, leads to a significant increase of the drift velocity.

Noteworthy is the estimate of the drift velocity in the dimensional units. Assuming that the particle is moving in the channel with period $L = 1$ $\mu$m filled with water at room temperature, with the dynamic viscosity of $10^{-3}$ kg/(m s), one finds from the simulations data that under optimal conditions the velocity can reach several tenths of a micron per second. In order of magnitude this compares reasonably well with the results obtained experimentally for molecular and artificial motors, as well as with those predicted in various theoretical studies of fluctuation-induced transport on the nanoscale [5,8,33].

### B. Resonant diffusion

In the present model, the nonequilibrium steady-state regime is characterized by a linear dependence of the variance of the particle's displacement, with the effective diffusion coefficient $\mathcal{D}$. An interplay of Brownian motion, space- and time-dependent geometric constraints gives rise to a nonmonotonic behavior of $\mathcal{D}$ versus the switching time $\tau$. The simulation results presented in Fig. 3 illustrate the dependence $\mathcal{D}(\tau)$ over several orders of magnitude in $\tau$, for a few choices of $b_+/b_-$ ($b_+/L = 0.25$ is fixed).

As evidenced from Fig. 3, the dependence $\mathcal{D}(\tau)$ bridges the two limits $\mathcal{D}(0)$ and $\mathcal{D}(\infty)$ by going through a broad resonance maximum. The limiting values can be evaluated using Eq. (8). Indeed, in the low-frequency regime, $\tau \to \infty$, the particle in each state is passing through many channel periods and thus has enough time to adjust to a new channel profile after each state flip. This suggests to write $\mathcal{D}(\infty)$ simply as the average between the values of effective diffusion coefficient calculated from Eq. (8) in the + and − states:

$$\mathcal{D}(\infty) = (\mathcal{D}_{\mathrm{FJ},+} + \mathcal{D}_{\mathrm{FJ},-})/2 = \left\{2\int_0^L w_+(x)\,dx/L \int_0^L 1/[w_+(x)D_+(x)]\,dx/L\right\}^{-1} + \left\{2\int_0^L w_-(x)\,dx/L \int_0^L 1/[w_-(x)D_-(x)]\,dx/L\right\}^{-1}, \tag{10}$$

with $D_\pm(x)$ defined in Eq. (9). Equation (10) is illustrated in Fig. 3 by the dashed lines for three values of $b_+/b_-$.

In the high-frequency regime, where $\tau$ is the shortest characteristic time scale, the particle jumps from one state to the other many times before being moved on an appreciable distance. So its position distributions in states + and − approach each other and a local equilibrium in a channel of the average width $w_0(x)$ is established. By analogy with the case of two-state fast fluctuating potential, the average static entropy potential (which the particle feels in this regime) can be written as $U_0(x) = [U_+(x) + U_-(x)]/2$, so that in view of Eq. (7) one gets

$$w_0(x) = \sqrt{w_+(x)w_-(x)}\,. \tag{11}$$

Then assuming the particle diffusion coefficient in this regime to be $D(0) = (D_+ + D_-)/2$, Eq. (8) takes the form

$$\mathcal{D}(0) = \left\{\int_0^L e^{-\beta[U_+(x)+U_-(x)]/2}\,dx/L \times \int_0^L e^{\beta[U_+(x)+U_-(x)]/2}/D_0(x)\,dx/L\right\}^{-1} = \left\{\int_0^L w_0(x)\,dx/L \int_0^L 1/[w_0(x)D_0(x)]\,dx/L\right\}^{-1}, \tag{12}$$

with the position-dependent diffusion coefficient $D_0(x) = \{1 + [dw_0(x)/dx]^2\}^{-1/3}$. Equation (12) is illustrated in Fig. 3 by the dash-dotted lines. Note that the following inequality holds $\mathcal{D}_{\mathrm{eff}}(\infty) > \mathcal{D}_{\mathrm{eff}}(0)$ for all values of $b_+/b_-$.

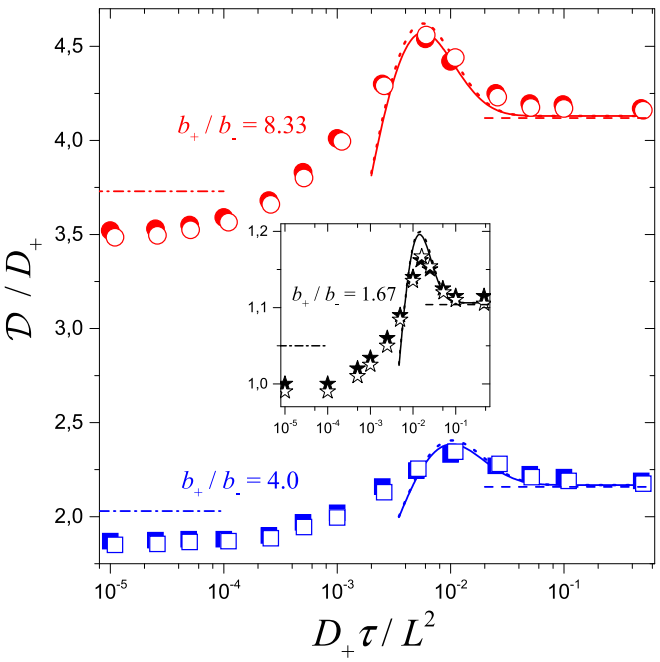


FIG. 3. Effective diffusion coefficient in units of $D_+$ vs. scaled switching time for different values of $b_+/b_-$ indicated by figures. The results obtained from 2D Brownian dynamics simulations for asymmetrical, $k_1 \neq k_2$, and symmetrical, $k_1 = k_2$, channel are marked by filled and empty symbols, respectively (the statistical error of the data is of the order of the symbol size). The solid and dotted lines are calculated from Eq. (21) for asymmetrical and symmetrical channel, respectively. The dashed and dashed-dotted lines show the limiting large-$\tau$ and small-$\tau$ values of the dimensionless effective diffusion coefficient calculated from Eqs. (10) and (12), respectively. The difference between these values in the symmetric and asymmetric channels is negligible. The inset compares numerical and analytical results for $b_+/b_- = 1.67$. The value of $b_+/L = 0.25$ is fixed; the dimensionless diffusion coefficients are $D_+ = 1$ and $D_- = b_+/b_-$.

As Fig. 3 clearly indicates, the stronger the oscillation amplitude, the more pronounced nonmonotonic behavior of $\mathcal{D}(\tau)$. The amplitude $A = b_+ - b_-$ affects not only the magnitude but also the position of the maximum. With its increase, the maximum is shifted toward shorter switching times, from $D_+\tau/L^2 = 0.016$ at $b_+/b_- = 1.67$ to $D_+\tau/L^2 = 0.006$ at $b_+/b_- = 8.33$. Comparison of Figs. 2 and 3 shows that the values of $\tau$ corresponding to the maximum positions of $\mathcal{D}(\tau)$ are few times larger than those of $v(\tau)$.

According to Fig. 3, the maximum value of the effective diffusion coefficient at $b_+/b_- = 8.33$ is $\mathcal{D} \approx 4.55$, which is almost identical with the diffusion coefficient of a particle moving freely one half of the observation time in state +, and the other half in state −, $D_0 = (D_+ + D_-)/2 \approx 4.66$. There can be, however, little doubt that for other geometric parameters than that used here one could achieve diffusion rates significantly larger than those for free diffusion. The basic physical mechanism for this selective diffusion enhancement is the optimal cooperation of spatially periodic gradients, time periodic modulation, and thermal noise, somewhat similar to the theoretical ideas expressed in articles [41].

Note that the difference between the data obtained in the symmetric and asymmetric channels is very small. Neither

the position, nor the magnitude of the $\mathcal{D}(\tau)$ peak are significantly influenced by the asymmetry. Thus, while the channel asymmetry plays a crucial role in the directed motion inducing mechanism (as demonstrated in the previous section), it affects only slightly the effect of the particle size oscillations on the rate of diffusion.

#### *Transport coherence*

As demonstrated above, the model at hand (in the asymmetric case) operates as a Brownian motor driven by the particle size oscillation. The directed motion of the motor is accompanied by diffusive spreading that may strongly obscure the rectification effect in systems with finite spatial extensions. The relative importance of drift to diffusion is quantified by the dimensionless Péclet number, $\mathrm{Pe} = |v|L/\mathcal{D}$ [47], where $v$ is the drift velocity, $\mathcal{D}$—the effective diffusion coefficient, and $L$ is a typical length scale (in our case the channel period). This number measures the transport coherence: the larger Pe, the more precision of the transport mechanism. Large values of the Péclet number, between 2 and 6, were reported in experiments on motor proteins, which indicates highly reliable operation of these molecular machines [48]. The transport coherence of simple flashing ratchet models relying only on a single particle dynamics was found quite low, with Péclet numbers always below 0.2 [47,49].

Based on the simulation data presented in Figs. 2 and 3, let us discuss the precision of the transport induced by the particle size oscillation. Both the velocity and the effective diffusivity are functions of the switching time and so does the Péclet number. The dependence of Pe on $\tau$ is very similar to that reported for the velocity: It exhibits a resonance-like behavior versus the switching time, vanishing in the small and large $\tau$ limits, and having a maximum in between. The position of its peak is determined by the amplitude of oscillation $A = b_+ - b_-$ and almost coincides with that of $v(\tau)$. The maximum values of the Péclet number are also determined by the amplitude $A$. More precisely, the larger $A$ (the smaller $b_-$), the greater the maximum values of Péclet number, $\mathrm{Pe}_m$. In particular, $\mathrm{Pe}_m \approx 0.03, 0.08$, and 0.12 for $b_+/b_- = 1.67, 4.0$, and 8.33, respectively. Certainly, greater (than these) values of $\mathrm{Pe}_m$ may be achieved by increasing $A$ and, especially, asymmetry of the channel. But, in any case, the transport in the considered model exhibits a low level of coherence, in agreement with the conclusion of previous work concerning reliability of operating mechanisms of simple flashing ratchets.

### C. Approximate analytical treatment

A promising way to elucidate the physical mechanisms underlying the particle transport is to treat the problem analytically. The conventional approach provides appropriate estimates of the effective diffusion coefficient only in the limits where the interstate transitions occurs either very slow or extremely fast, Eqs. (10) and (12), and the drift velocity vanishes. To clarify the nonmonotonic behavior of $v(\tau)$ and $\mathcal{D}(\tau)$ between these limits, we suggest an approximate analytical description. It extends our previous analysis [26] to incorporate resonant diffusion due to a time variation of particle size. The derivation of the main equations relies on several heuristic assumptions. The validity, accuracy, and range of applicability of this description are verified by the simulation results.

#### *1. Basic assumptions*

(i) The conditions of the particle motion are essentially different in the alternate states provided the interstate switching proceeds not too fast. This suggests to treat the particle dynamics in the + and − states in a different manner.

(ii) The + state is characterized by relatively narrow channel width, relatively small effective bottlenecks, and relatively slow diffusion. It is supposed that in this state the particle executes an unbiased diffusive motion in the entropy potential $U_+(x)$ with the effective diffusion coefficient $\mathcal{D}_{\mathrm{FJ},+}$ given by Eq. (8). The + state makes negligible contribution to the drift and serves solely to form an asymmetric particle distribution along the $x$-axis, $\rho_+(x)$, assumed to be proportional to $w_+(x)$ defined in Eq. (3), i.e.,

$$\rho_+(x) = w_+(x)/\Omega, \quad \Omega = \int_0^L w_+(x)\,dx. \tag{13}$$

(iii) We assume that immediately after transition to the − state, the particle diffuses freely because it is being located far away from the channel boundary [in view of the inequality $w_-(x) > w_+(x)$]. Then the probabilities that after time $\tau$ the particle initially (when the transition to the − state occurs) at point $x$, $0 < x < L$, escapes from a given unit cell to the right and to the left can be estimated as follows:

$$\begin{aligned} p(x,\tau) &= \tfrac{1}{2}\,\mathrm{erfc}[(L-x)/\sqrt{4D_-\tau}], \\ q(x,\tau) &= \tfrac{1}{2}\,\mathrm{erfc}(x/\sqrt{4D_-\tau}). \end{aligned} \tag{14}$$

It is instructive to map the continuous particle dynamics in the − state into a discrete random walk process along the $x$ axis in which the walker is allowed to jump on the distance $l$ to the right or to the left, or to remain in the same site, the duration of each step being $\tau$. Let the probabilities of these events be

$$p(\tau) = \int_0^L p(x,\tau)w_+(x)\,dx, \quad q(\tau) = \int_0^L q(x,\tau)w_+(x)\,dx, \tag{15}$$

and $o(\tau) = 1 - p(\tau) - q(\tau)$, respectively. Then the mean and variance per step time interval $\tau$ of the walker displacement read

$$\begin{aligned} \lambda_{\mathrm{rw}}(\tau) &= l[p(\tau) - q(\tau)], \\ \epsilon^2_{\mathrm{rw}}(\tau) &= l^2\{p(\tau) + q(\tau) - [p(\tau) - q(\tau)]^2\}. \end{aligned} \tag{16}$$

(iv) The description of the particle motion in the − state in terms of the 1D random walks formulated above is justified at times, when the particle feels no confinement. This approximation fails as the particle approaches the channel wall and the steady state distribution $\rho_+(x)$ transforms into a new one. To improve the estimates given in Eq. (16), it is necessary to account for the effect of transverse diffusion on the longitudinal displacement. The simplest (though not most convincing) way to do this is to introduce a single exponential attenuation factor, $e^{-t/t_{\mathrm{rel}}}$, which reduces the system response, as confinement effects become more and more significant. More specifically, the mean and variance per step of the

displacement predicted by Eq. (16) should be corrected by multiplication with the factor $e^{-t/t_{\rm rel}}$. A crude estimate for the relaxation time is [26]

$$t_{\rm rel} = \frac{4b_-(a-b_+)(1-b_-/b_+)}{3D_+}. \tag{17}$$

(v) We suppose that when the particle distribution reaches a stationary one in the $-$ state, its motion can be considered as an unbiased diffusion in the entropy potential $U_-(x)$ with the effective diffusion coefficient $\mathcal{D}_{\rm FJ,-}$ given by Eq. (8). Moreover, we assume that this mechanism comes into play gradually, leading to the mean square displacement for time interval $\tau$ equal to $2\tau\mathcal{D}_{\rm FJ,-}(1-e^{-t/t_{\rm rel}})$.

#### 2. *Expressions for the drift velocity and effective diffusion coefficient*

The definitions of the drift velocity and effective diffusion coefficient given in Eqs. (5) and (6) can be rewritten in terms of the mean and variance of the particle displacement for the period $2\tau$, $\lambda(\tau)$ and $\epsilon^2(\tau)$, respectively:

$$v(\tau) = \frac{\lambda(\tau)}{2\tau}, \quad \mathcal{D}(\tau) = \frac{\epsilon^2(\tau)}{4\tau}. \tag{18}$$

With these definitions and the assumptions formulated above, approximate formulas for the desired quantities can be easily obtained.

The only contribution to the mean displacement comes from the particle motion in the $-$ state, i.e., $\lambda(\tau) \simeq \lambda_{\rm rw}(\tau)$. Then for the drift velocity we get

$$v(\tau) = \frac{l}{2\tau}\, e^{-\tau/t_{\rm rel}}\,[p(\tau)-q(\tau)]. \tag{19}$$

The total variance of the displacement for the period consists of several contributions due to the various sources discussed above. By summing up all these variances, we obtain

$$\epsilon^2(\tau) = e^{-\tau/t_{\rm rel}}\epsilon^2_{\rm rw}(\tau) + 2\tau[(1-e^{-\tau/t_{\rm rel}})\mathcal{D}_{\rm FJ,-} + \mathcal{D}_{\rm FJ,+}]. \tag{20}$$

Then, according to its definition given in Eq. (18), the effective diffusion coefficient can be written as follows

$$\mathcal{D}(\tau) = \frac{l^2}{4\tau}\, e^{-\tau/t_{\rm rel}}\{p(\tau)+q(\tau)-[p(\tau)-q(\tau)]^2\} + [(1-e^{-\tau/t_{\rm rel}})\mathcal{D}_{\rm FJ,-} + \mathcal{D}_{\rm FJ,+}]/2. \tag{21}$$

The probabilities $p(\tau)$ and $q(\tau)$ entering into the final expressions Eqs. (19) and (21) are defined by Eqs. (13)–(15). The diffusion coefficients $\mathcal{D}_{\rm FJ,\pm}$ are found from Eqs. (8) and (9). The step-length $l$ is taken to be scaled to the channel period $L$, i.e., $l = \alpha L$, where $\alpha$ is an adjustable dimensionless parameter (of order unity) fixed by comparing with the simulation data.

The derivation of Eqs. (19) and (21) is based on several physically reasonable assumptions rather than on strict mathematical proof. Nevertheless, as it easy to see, both equations correctly reproduce the main qualitative features of the quantities of interest. In particular, it follows from Eq. (19) that the drift velocity: (1) disappears in a symmetric channel, $k_1 = k_2$, as well as in the absence of size oscillation, $b_+ = b_-$, and with the effective bottleneck size, $a - b_+$, approaching zero; (2) exhibits a nonmonotonic behavior versus the switching time, vanishing in the low- and high-frequency limits, and having a maximum in between; (3) is directed toward the steeper wall of the channel. The appearance of a peak in the dependence $v(\tau)$ may be interpreted as a kind of resonance between the periodic stimulus and the system response. The particle drift is produced most effectively when the switching time $\tau$ matches the characteristic time of the system response (discussed in detail in Sec. III B 2 in our previous work [26]).

Equation (21) predicts a nonmonotonic behavior of $\mathcal{D}(\tau)$ if the particle size varies in time, $b_+ \neq b_-$ and the largest particle radius is smaller than the bottleneck radius $a$. This dependence approaches two plateau values at slow and fast switching frequency, and has a broad maximum in between. While the large $\tau$ plateau coincides with that predicted by Eq. (10), the small $\tau$ plateau value drawn from Eq. (21) proves to be much less than the value given by expression (12). The latter is not a surprise, since in the fast switching regime the assumptions formulated in the previous section [especially (i) and (ii)] fail and the description outlined above becomes inadequate. At the same time, it should be noted that at slow and intermediate switching frequencies Eq. (21) provides a satisfactory description of the effective diffusivity, as demonstrated in the next section.

### D. Analytical versus simulation results

Equations (19) and (21) provide an approximate analytical description of the particle transport in the channel, induced by oscillation of the particle size. To assess its relevance, accuracy, and range of applicability, this description should be verified by the simulations results.

Figure 2 illustrates Eq. (19) (recast in dimensionless form, with $\alpha$ taken to be 0.5) for several values of $b_+/b_-$ and compares its predictions to the results for the drift velocity obtained from Brownian dynamics simulations. As one would expect, at small and large $\tau$, where the effect is very weak, the accuracy of Eq. (19) is quite low since the approximations made in its derivation are too coarse in this range of $\tau$. However, the analytical results provided by this equation agree satisfactorily with the numerical ones in the most interesting range of $\tau$, where the velocity takes its maximum values and the particle drift is most evident. The smaller $b_-$, the better agreement is seen. As Fig. 2 clearly indicates, Eq. (19) yields sensible predictions for the position and magnitude of the peak of $v(\tau)$ at different values of $b_+/b_-$. In accordance with the simulations results, the position of the peak shifts to smaller $\tau$ and its magnitude grows as the radius $b_-$ decreases. Moreover, a more extended analysis [26] gives evidence that Eq. (19) leads to appropriate quantitative estimates of the position and magnitude of the peak.

Figure 3 compares the dependence of the effective diffusivity on the switching time as calculated from Eq. (21) (recast in dimensionless form, with $\alpha$ taken to be 0.5) with that obtained from the simulations for a few values of $b_+/b_-$. Additionally, the large- and small $\tau$ asymptotic values of $\mathcal{D}(\tau)$ determined by Eqs. (10) and (12), respectively, are shown in this figure. As can be seen, the large $\tau$ plateau value, Eq. (10), agrees quite well with the results obtained in simulations for all considered values of $b_+/b_-$. The approximations involved

in the derivation of Eq. (12) describing the opposite limit are less reliable. This is why the small $\tau$ limit is predicted not so accurate as that at large $\tau$. As the comparison with the simulation data shows, Eq. (12) gives an overestimate of $\mathcal{D}(0)$, but the relative mistake does not exceed 10%.

The solid and dotted lines in Fig. 3 illustrate Eq. (21) in the asymmetric and symmetric cases, respectively. Note that the influence of the channel asymmetry on the effective diffusivity is weak, in agreement with that observed in the simulations. At large $\tau$ Eq. (21) is reduced to Eq. (10), so that it provides a good fit to the simulations. At intermediate values of $\tau$ the agreement with the simulations data is quite satisfactory. In particular, this equation yields reasonable predictions in the $\tau$ range, where the dependence $\mathcal{D}(\tau)$ exhibits the resonant behavior. The position of the peak shifts to smaller $\tau$ and its magnitude grows as the radius $b_-$ decreases, in agreement with that observed in the simulations. As already noted, at small $\tau$ Eq. (21) fails to reproduce the correct behavior of $\mathcal{D}(\tau)$. For this reason, the left-hand branches of the curves are not shown in Fig. 3.

Thus, summing up the comparison results, it can be stated that the approximate description of the particle transport given by Eqs. (19) and (21) is not only qualitatively correct, but also in semi-quantitative agreement with the results obtained from the simulations, except the range of small switching times. So the proposed approach provides a satisfactory way to handle the problem analytically.

## IV. CONCLUSIONS

The present paper is devoted to nonequilibrium particle transport along the channel, schematically shown in Fig. 1, resulting from periodical switching of the particle size between two values. We have demonstrated that the combined action of spatiotemporal variation of the entropy potential and thermal noise essentially affects the transport properties of the system. The two main observations are: emergence of the particle drift (in case of asymmetric channel) and resonant diffusion, both of purely entropic origin.

The drift induced by the particle size oscillation exhibits a resonance-like behavior with respect to the switching time (see Fig. 2). It approaches zero both for fast and slow switching between states, and has a maximum in between, when the period of the size oscillation matches the characteristic time of the system response. The larger the amplitude of the input signal, the greater the drift velocity. The oscillation of the particle diffusion coefficient accompanying the oscillation of the particle size leads to significant enhancement of the effect.

The dependence of the effective diffusion coefficient on the switching time bridges the limits of slow and fast size modulation, estimated by Eqs. (10) and (12), by going through a broad resonance maximum (see Fig. 3). For optimal geometric parameters one could achieve diffusion rates exceeding those for free diffusion, providing selective enhancement of the process. The basic physical mechanism for this resonant-like behavior is the cooperation of spatially periodic gradients, time periodic modulation, and thermal noise. The stronger the size oscillation amplitude, the more pronounced this nonmonotonic behavior. The oscillation amplitude affects not only the magnitude but also the position of the maximum. While the channel asymmetry plays a crucial role in the drift inducing mechanism, it has only insignificant influence on the rate of diffusion. The directed motion induced by the particle size variation exhibits a low level of coherence, in agreement with the conclusion of previous studies concerning reliability of operating mechanisms of simple flashing ratchets.

The effects detected in the present work require an analytical description beyond the FJ theory. We have proposed an approximate analytical treatment to clarify the simulation results. The derivation of the expressions for the drift velocity and the effective diffusivity, Eqs. (19) and (21), relies on a few intuitive arguments capturing the main physics of the model. Comparison of the analytical predictions and the numerical results (see Figs. 2 and 3) has shown that Eqs. (19) and (21) qualitatively reproduce all features of the process. Moreover, they are found to be in satisfactory quantitative agreement, except the high-frequency switching regime. Thus, the proposed approach provides a simple, satisfactory tool to handle the problem analytically.

Systems, where geometrically restricted diffusion is coupled with a time variation of the particle size, can potentially be realized experimentally. We hope that our theoretical work may stimulate experimental research on transport properties of such systems.

## ACKNOWLEDGMENT

This work was carried out within the State Program of TIPS RAS.

[1] J. Kärger and D. M. Ruthven, *Diffusion in Zeolites and Other Microporous Solids* (Wiley, New York, 1992); D. Hillel, *Fundamentals of Soils Physics* (Academic Press, New York, 1980).

[2] B. Hille, *Ion Channels in Excitable Membranes* (Sinauer Associates, Sunderland, 2001).

[3] D. Reguera, A. Luque, P. S. Burada, G. Schmid, J. M. Rubí, and P. Hänggi, Phys. Rev. Lett. **108**, 020604 (2012); T. Motz, G. Schmid, P. Hänggi, D. Reguera, and J. M. Rubí, J. Chem. Phys. **141**, 074104 (2014).

[4] W. M. Saltzman, *Drug Delivery: Engineering Principles for Drug Therapy* (Oxford University Press, Oxford, 2001).

[5] P. C. Bressloff and J. M. Newby, Rev. Mod. Phys. **85**, 135 (2013).

[6] F. Marchesoni and S. Savel'ev, Phys. Rev. E **80**, 011120 (2009).

[7] G. Schmid, P. S. Burada, P. Talkner, and P. Hänggi, Adv. Solid State Phys. **48**, 317 (2009); J. M. Rubí and D. Reguera, Chem. Phys. **375**, 518 (2010); L. Dagdug, A. M. Berezhkovskii, Yu. A. Makhnovskii, V. Yu. Zitserman, and S. M. Bezrukov, J. Chem. Phys. **136**, 214110 (2012).

[8] P. Hänggi and F. Marchesoni, Rev. Mod. Phys. **81**, 387 (2009).

[9] P. S. Burada, P. Hänggi, F. Marchesoni, G. Schmid, and P. Talkner, Chem. Phys. Chem. **10**, 45 (2009).

[10] P. Malgaretti, I. Pagonabarraga, and J. M. Rubí, Front. Phys. **1**, 21 (2013).

[11] S. Matthias and F. Müller, Nature **424**, 53 (2003); C. Marquet, A. Buguin, L. Talini, and P. Silberzan, Phys. Rev. Lett. **88**, 168301 (2002); K. Mathwig, F. Müller, and U. Gösele, New J. Phys. **13**, 033038 (2011); S. Pagliara, S. L. Dettmer, K. Misiunas, L. Lea, Y. Tan, and U. F. Keyser, Eur. Phys. J. Special Topics **223**, 3145 (2014).

[12] X. Yang, C. Liu, Y. Li, F. Marchesoni, P. Hänggi, and H. P. Zhang, Proc. Natl. Acad. Sci. USA **114**, 9564 (2017).

[13] D. Lairez, M.-C. Clochard, and J.-E. Wegrowe, Sci. Rep. **6**, 38966 (2016).

[14] R. Zwanzig, J. Phys. Chem. **96**, 3926 (1992).

[15] D. Reguera and J. M. Rubí, Phys. Rev. E **64**, 061106 (2001).

[16] S. Martens, I. M. Sokolov, and L. Schimansky-Geier, J. Chem. Phys. **136**, 111102 (2012); P. K. Ghosh, P. Hänggi, F. Marchesoni, F. Nori, and G. Schmid, Phys. Rev. E **86**, 021112 (2012); P. K. Radtke and L. Schimansky-Geier, *ibid.* **85**, 051110 (2012).

[17] D. Reguera, G. Schmid, P. S. Burada, J. M. Rubí, P. Reimann, and P. Hänggi, Phys. Rev. Lett. **96**, 130603 (2006); S. Martens, G. Schmid, L. Schimansky-Geier, and P. Hänggi, Chaos **21**, 047518 (2011).

[18] F. Marchesoni, J. Chem. Phys. **132**, 166101 (2010); L. Bosi, P. K. Ghosh, and F. Marchesoni, *ibid.* **137**, 174110 (2012).

[19] A. M. Berezhkovskii, L. Dagdug, Yu. A. Makhnovskii, and V. Yu. Zitserman, J. Chem. Phys. **132**, 221104 (2010); Yu. A. Makhnovskii, A. M. Berezhkovskii, L. V. Bogachev, and V. Yu. Zitserman, J. Phys. Chem. B **115**, 3992 (2011); M. Borromeo and F. Marchesoni, Chem. Phys. **375**, 536 (2010).

[20] Yu. A. Makhnovskii, A. M. Berezhkovskii, and V. Yu. Zitserman, Chem. Phys. **367**, 110 (2010); M. Mangeat, T. Guérin, and D. S. Dean, Europhys. Lett. **118**, 40004 (2017); J. Chem. Phys. **149**, 124105 (2018).

[21] S. Martens, G. Schmid, A. V. Straube, L. Schimansky-Geier, and P. Hänggi, Eur. Phys. J. Special Topics **222**, 2453 (2013); B. Golshaei and A. Najafi, Phys. Rev. E **91**, 022101 (2015); B. H. Bradshaw-Hajek, N. Islam, S. J. Miklavcic, and L. R. White, J. Eng. Math. **111**, 1 (2018).

[22] B.-Q. Ai and L.-G. Liu, Phys. Rev. E **74**, 051114 (2006); B.-Q. Ai, *ibid.* **80**, 011113 (2009); R. Wang, J.-N. Zhou, X.-M. Liu, and H. Xiao, Int. J. Mod. Phys. B **29**, 1550026 (2015).

[23] V. Yu. Zitserman, A. M. Berezhkovskii, A. E. Antipov, and Yu. A. Makhnovskii, J. Chem. Phys. **135**, 121102 (2011); Yu. A. Makhnovskii, V. Yu. Zitserman, and A. E. Antipov, Zh. Eksp. Teor. Fiz. **142**, 603 (2012) [JETP **115**, 535 (2012)].

[24] B.-Q. Ai and L.-G. Liu, Chem. Phys. **344**, 185 (2008); B.-Q. Ai, J. Chem. Phys. **131**, 054111 (2009).

[25] H. Ding, H. Jiang, and Z. Hou, J. Chem. Phys. **143**, 244119 (2015); M. F. Carusela and J. M. Rubí, *ibid.* **146**, 184901 (2017); J. Phys.: Condens. Mattter **30**, 244001 (2018).

[26] Yu. A. Makhnovskii, S.-Y. Sheu, D.-Y. Yang, and S. H. Lin, J. Chem. Phys. **146**, 154103 (2017).

[27] V. Yu. Zitserman, Yu. A. Makhnovskii, L. I. Trakhtenberg, D.-Y. Yang, and S. H. Lin, Pis'ma Zh. Eksp. Teor. Fiz. **105**, 315 (2017) [JETP Lett. **105**, 335 (2017)].

[28] P. K. Ghosh, V. R. Misko, F. Marchesoni, and F. Nori, Phys. Rev. Lett. **110**, 268301 (2013); J.-C. Wu, Q. Chen, and B.-Q. Ai, Phys. Lett. A **379**, 3025 (2015); J.-C. Wu and B.-Q. Ai, Sci. Rep. **6**, 24001 (2016); P. Malgaretti and H. Stark, J. Chem. Phys. **146**, 174901 (2017).

[29] P. Malgaretti, I. Pagonabarraga, and J. M. Rubí, Phys. Rev. E **85**, 010105 (2012); J. Chem. Phys. **138**, 194906 (2013); Q. Chen, B.-Q. Ai, and J.-W. Xiong, Chaos **24**, 033119 (2014).

[30] L. Dagdug, A. M. Berezhkovskii, Yu. A. Makhnovskii, and V. Yu. Zitserman, J. Chem. Phys. **129**, 184706 (2008); K.-L. Cheng, Y.-J. Sheng, and H.-K. Tsao, *ibid.* **129**, 184901 (2008); W. Riefler, G. Schmid, P. S. Burada, and P. Hänggi, J. Phys.: Condens. Matter **22**, 454109 (2010).

[31] B.-Q. Ai and J.-C. Wu, J. Chem. Phys. **139**, 034114 (2013); M. Bruna and S. J. Chapman, Bull. Math. Biol. **76**, 947 (2014).

[32] D. Mondal and M. Muthukumar, J. Chem. Phys. **145**, 084906 (2016); V. Bianco and P. Malgaretti, *ibid.* **145**, 114904.

[33] M. Motornov, Y. Roiter, I. Tokarev, and S. Minko, Prog. Polym. Sci. **35**, 174 (2010); S. Erbas-Cakmak, D. A. Leigh, C. T. McTernan, and A. L. Nussbaumer, Chem. Rev. **115**, 10081 (2015); C. Cheng and J. F. Stoddart, Chem. Phys. Chem. **17**, 1780 (2016).

[34] D. Shi, M. Matsusaki, T. Kaneko, and M. Akashi, Macromolecules **41**, 8167 (2008).

[35] H.-J. Zhang, Y. Xin, Q. Yan, L.-L. Zhou, L. Peng, and J.-Y. Yuan, Macromol. Rapid Commun. **33**, 1952 (2012).

[36] J. Hu, H. Yu, L. H. Gan, and X. Hu, Soft Matter **7**, 11345 (2011).

[37] R. D. Astumian and M. Bier, Phys. Rev. Lett. **72**, 1766 (1994).

[38] S. Lifson and J. L. Jackson, J. Chem. Phys. **36**, 2410 (1962); R. Festa and E. G. d'Agliano, Physica A **90**, 229 (1978); L. Gunther, M. Revzen, and A. Ron, *ibid.* **95**, 367 (1979); D. L. Weaver, *ibid.* **98**, 359 (1979).

[39] R. L. Stratonovich, Radiotekh. Elektron. (Moscow) **3**, 497 (1958) [English translation in *Non-linear Transformations of Stochastic Processes*, edited by P. I. Kuznetsov, R. L. Stratonovich, and V. I. Tikhonov (Pergamon Press, Oxford, 1965)].

[40] P. Reimann, C. Van den Broeck, H. Linke, P. Hänggi, J. M. Rubí, and A. Pérez-Madrid, Phys. Rev. Lett. **87**, 010602 (2001); B. Lindner, M. Kostur, and L. Schimansky-Geier, Fluct. Noise Lett. **1**, R25 (2001); P. S. Burada, G. Schmid, and P. Hänggi, Philos. Trans. R. Soc. A **367**, 3157 (2009).

[41] H. Gang, A. Daffertshofer, and H. Haken, Phys. Rev. Lett. **76**, 4874 (1996); D. Reguera, P. Reimann, P. Hänggi, and J. M. Rubí, Europhys. Lett. **57**, 644 (2002); A. A. Dubkov and B. Spagnolo, Phys. Rev. E **72**, 041104 (2005); M. Borromeo and F. Marchesoni, *ibid.* **78**, 051125 (2008); P. Romanczuk, F. Müller, and L. Schimansky-Geier, *ibid.* **81**, 061120 (2010).

[42] S. Bleil, P. Reimann, and C. Bechinger, Phys. Rev. E **75**, 031117 (2007); W. C. Germs, E. M. Roeling, L. J. van IJzendoorn, R. A. J. Janssen, and M. Kemerink, Appl. Phys. Lett. **102**, 073104 (2013).

[43] M. Y. Jaffrin and A. H. Shapiro, Annu. Rev. Fluid Mech. **3**, 13 (1971); J. V. Ramanamurthy, K. M. Prasad, and V. K. Narla, Phys. Fluids **25**, 091903 (2013).

[44] Y. Cávez, G. Chacón-Acosta, and L. Dagdug, J. Phys.: Condens. Matter **30**, 194001 (2018).

[45] In dimensionless notations, all lengths are scaled by the length of the period $L$ and all times are scaled by the characteristic diffusion time of the particle in the $+$ state, $\tau_D = L^2/D_+$. The dimensionless values of the diffusion coefficients and

the velocity are set as follows: $\hat{D}_+ = 1$, $\hat{D}_- = b_+/b_-$, and $\hat{v} = v/(D_+/L)$.

[46] G. Marsaglia and W. W. Tsang, J. Stat. Software **5**, 1 (2000).

[47] J. A. Freund and L. Schimansky-Geier, Phys. Rev. E **60**, 1304 (1999).

[48] K. Visscher, M. J. Schnitzer, and S. M. Block, Nature (London) **400**, 184 (1999); H. R. Khataee and A. R. Khataee, Nano **5**, 13 (2010).

[49] Y. Zhou and J.-D. Bao, Physica A **343**, 515 (2004).